Available online at www.sciencedirect.com
ScienceDirect
Journal of Hazardous Materials 156 (2008) 135–140
Journal of Hazardous Materials
www.elsevier.com/locate/jhazmat

Preparation and characterization of N–S-codoped TiO_2 photocatalyst and its photocatalytic activity

Fengyu Wei [a,b,*], Liangsuo Ni [a], Peng Cui [a,b]

[a] School of Chemical Engineering, Hefei University of Technology, Hefei 230009, PR China
[b] Anhui Key Laboratory of Controllable Chemical Reaction & Material Chemical Engineering, Hefei, 230009, PR China

Received 25 June 2007; received in revised form 3 December 2007; accepted 4 December 2007
Available online 15 December 2007

Abstract

N–S-codoped anatase nanosized TiO_2 photocatalyst (NSTO) was successfully prepared by one-step hydrothermal method from a mixed aqueous solution of $Ti(SO_4)_2$ and thiourea. The samples were characterized by XRD, UV–vis, XPS, FT-IR and EA. From results of UV–vis, a red shift of the absorption edge was brought out owing to N and S codoping, and the extension for photoabsorption range of NSTO occurred. XRD, XPS, EA and FT-IR studies revealed that N and S were in situ codoped in the lattice of TiO_2 and N concentration decreased from the surface to the center of NSTO. Especially, the photocatalytic tests indicated that NSTO exhibited a high activity for decompositions of methyl orange both under UV-light and vis-light irradiation comparing to S-doped TiO_2 (STO) and undoped TiO_2 (TO). The high activity of NSTO can be related to the results of the synergetic effects of strong absorption in the UV–vis region, red shift in adsorption edge, oxygen vacancies and the enhancement of surface acidity induced by N and S codoping.

Keywords: N and S codoping; Titanium dioxide; UV–vis photocatalytic activity; Hydrothermal method

1. Introduction

Titania is the most widely used photocatalyst in photodegradation of organic pollutants in air and water [1–2]. However, TiO_2 can be activated only under UV-light irradiation due to its large band gap value of 3.2 eV. Therefore, it is indispensable to develop a TiO_2 photocatalyst with a high level of activity under visible light. In the past, transition metal cations have been used as dopants to red shift the absorption edge of TiO_2 to a visible-light region [3–5]. Recently, C, N, S, F, B anion-doped TiO_2 photocatalysts that show a relatively high level of activity under visible-light irradiation have been reported [6–12]. These non-metal elements have been proved to be beneficial doping elements in the TiO_2 through mixing their p orbital with O2p orbital to reduce the band gap energy of TiO_2. In order to further improve the photocatalytic activity, codoped titania with double non-metal elements has attracted more attention. N–F-codoped TiO_2 powders synthesized by spray pyrolysis showed the highest visible-light activity for decompositions of both acetaldehyde and trichloroethylene [13]. They also demonstrated that the high activity was ascribed to a synergetic consequence of several beneficial effects induced by the N–F codoping. Ohno et al. [14] confirmed that the photocatalytic activity levels of C, S cation-codoped $SrTiO_3$ were about two times higher than those of undoped $SrTiO_3$ under a wide range of light irradiation at wavelengths longer than 350 nm. N/S-codoped titania photocatalyst $TiO_{2-x}A_y$ (A = N, S) was prepared by hydrothermal treatment using $TiCl_3$ solutions with various nitrogen sources, which exhibited excellent visible-light absorption and photocatalytic ability for the oxidative destruction of nitrogen monoxide [15]. Liu and Gao [16] had synthesized (S, N)-codoped rutile-TiO_2 photocatalyst using a hydrothermal method and subsequent nitridation under NH_3 flow at 873 K for 4 h. Yu et al. [17] had developed N, S-codoped TiO_2 by hydrolysis of $Ti(SO_4)_2$ in a $NH_3{\cdot}H_2O$ solution. They demonstrated that the photocatalytic activity of the as-prepared TiO_2 powders calcined at a temperature range of 400–700°C are obviously higher than that of P25. However, the effect of S, N codoping on the UV-light

* Corresponding author at: School of Chemical Engineering, Hefei University of Technology, Hefei 230009, PR China. Tel.: +86 5512901458; fax: +86 5512901450.
E-mail address: weifyliuj@yahoo.com.cn (F. Wei).

0304-3894/$ – see front matter © 2008 Elsevier B.V. All rights reserved.
doi:10.1016/j.jhazmat.2007.12.018

photocatalytic activity of TiO_2 had not been mentioned yet, and most methods are high-temperature processes, using expensive precursors or preparation instruments.

Hydrothermal method is very simple and does not require any special equipment. TiO_2 prepared by this method have well-crystalline phase and small crystalline size, which benefit to thermal stability and photocatalytic activity [18]. In this work, a single anatase phase of N–S-codoped TiO_2 photocatalyst had been prepared by a one-step low-temperature hydrothermal method using cheaper material $Ti(SO_4)_2$ as Ti source, thiourea as nitrogen and sulfur sources. This work is very helpful for preparing a novel UV–vis photoactive TiO_2 powders which may have a wide variety of practical applications.

2. Experimental

2.1. Synthesis

The N, S-codoped TiO_2 (called NSTO) was synthesized by hydrothermal method. A mixed aqueous solution of $Ti(SO_4)_2$ (0.6 M, 30 mL) and thiourea (1.37 g) was placed into a Teflon-lined stainless steel autoclave of 50 mL capacity, carried out at 130 °C for 20 h. The produced powders were separated by centrifugation, washed with deionized water 3–4 times to make the precipitate free of SO_4^{2-}, as tested using $BaSO_4$ solution, then dried at 90 °C for 24 h. For comparison, only S-doped TiO_2 (called STO) was synthesized by the same method using 0.6 M $Ti(SO_4)_2$ 30 mL and 0.1 M H_2SO_4 5 mL. Undoped TiO_2 (called TO) was synthesized as above only using 0.6 M $Ti(SO_4)_2$ as starting materials.

2.2. Characterization

The crystal structure of the products was determined by using an X-ray diffractometer (Rigaku, D/Max-rB) with a Cu Kα radiation. The binding energy was identified by X-ray photoelectron spectroscopy (XPS) using a VG ESCALAB-MK photoelectron spectrometer with an Mg Kα source. The shift of binding energy due to relative surface charging was corrected using the C1s level at 284.8 eV as an internal standard. The absorption edge and band gap energy of the samples were measured using a Shimadzu UV-240 spectrophotometer equipped with a diffuse reflectance accessory. Element analysis was identified by Elemental Vario EL-III. FT-IR spectra on KBr pellets of the samples were recorded on a PE-100 FT-IR spectrometer at a resolution of 4 cm^{-1}. Intensity of sunlight was determined by Digital Illuminance Meter (TES Electrical Electronic Corp., TES-1335, China).

2.3. Measurement of photocatalytic activity

The photocatalytic activity of the as-prepared TiO_2 powders was evaluated by measuring the decomposition of 10 mg/L methyl orange (MO) aqueous solution. The UV photocatalytic reactions were carried out in a glass immersion photochemical reactor charged with 800 mL methyl orange aqueous solution; the used amount of catalyst was 0.1 g. An air flow was employed to produce a homogenous suspension of the catalyst in the solution, an 18 W low-pressure mercury lamp as UV-light source. The vis-light photocatalytic experiments were carried out in a dish of about 15 cm diameter using sunlight as visible-light source. Three hundred milliliters methyl orange suspension was stirred magnetically. Prior to photocatalytic experiment, the catalysts were settled in suspension for 30 min in the dark for the adsorbtion equilibrium. The concentrations of methyl orange solution were quantified by a 722P spectrophotometer (China) at 464 nm, or using a Shimadzu UV-2550 (Japan) spectrophotometer.

In a heterogenous solid–liquid reaction, the photocatalytic reaction on the surface of TiO_2 powders is a pseudo-first-order reaction and its kinetic equation may be expressed as follows [1]:

$$r = -\frac{dc}{dt} = kc \quad (1)$$

where k is the apparent rate constant of pseudo-first-order. So, the decrease of MO concentration will follow the arithmetical progression proportion. The rate equation is

$$\ln\frac{c}{c_0} = -kt \quad (2)$$

where c_0 and c represent the initial equilibrium concentration and reaction concentration of reactant, respectively.

3. Results and discussion

3.1. Phase structure

The XRD patterns (Fig. 1) show that the homogeneous anatase phase was formed in the as-prepared samples. The anatase TiO_2 is very beneficial for photocatalytic degradation of organic contamination [18]. According to Debye–Scherrer and Bragg law, the crystallite size and unit cell parameters were summarized in Table 1. From Table 1 it is obtained that the crystallite growth of STO or NSTO is strongly restrained during the hydrothermal treatment, which results in a slight broadening in XRD peaks. The unit cell parameters of STO remained almost unchanged, indicating that S is not weaved into the crystal struc-

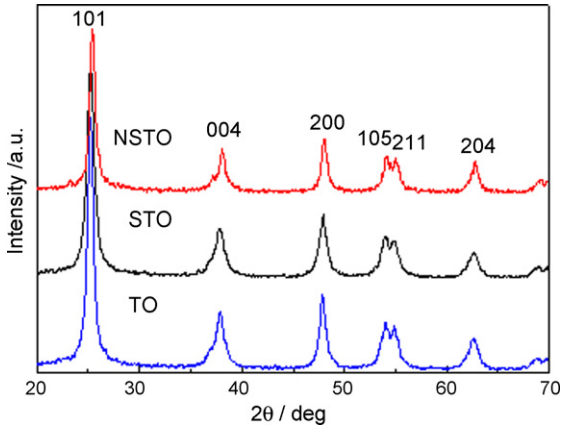

Fig. 1. XRD patterns of the as-prepared TiO_2 powders.

Table 1
Some characteristics of samples

Sample	Crystallite size (nm)	Unit cell parameters		
		a (nm)	*c* (nm)	*v* (nm^3)
[a]TiO_2		3.7852	9.5139	136.3127
TO	20.5	3.8000	9.4571	136.5603
STO	12.9	3.8020	9.4648	136.8162
NSTO	16.2	3.7960	9.6803	139.4898

[a] JCPDS no. 21-1272.

ture of the sample. However, the unit cell parameters of NSTO are affected greatly, which means that S and N codoped into the lattice of TiO_2. Those results also mean that the chemical states of S atom into NSTO and STO are in the different forms.

3.2. UV–vis diffuse reflectance spectra

The diffuse reflectance spectra of the as-prepared samples are shown in Fig. 2. It is obvious that the absorption of NSTO in the UV–vis region is stronger than that of STO and TO, the absorption of STO is stronger than that of TO. The onset absorption spectrum of NSTO shows a red shift. The enhancement of absorbance in the UV–vis region increases the number of photogenerated electrons and holes to participate in the photocatalytic reaction, which can enhance the photocatalytic activity of TiO_2 [12]. Lettmann et al. [19] reported that there is a good correlation between the light absorption properties and the photocatalytic activity, so it is a good way to obtain high vis photocatalytic activity by improving its photoabsorption.

3.3. XPS and EA analysis

The chemical forms and content of the N and S element in NSTO were investigated through XPS. Fig. 3 shows the XPS survey spectrum of NSTO. Atomic ratio of Ti:O:N:S is 1:1.95:0.017:0.06 determined by the XPS. Oxygen vacancies emerge in NSTO because of the rate of O/Ti <2.

The high-resolution N1s XPS spectrum of NSTO (Fig. 4) shows that N1s region can be fitted into four peaks in the spectrum around 396, 400, 401.5 and 402.2 eV. The peak detected

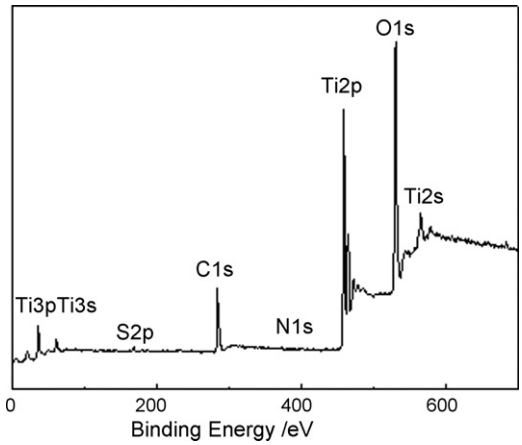

Fig. 3. XPS spectrum of NSTO.

at 396 eV was assigned to an atomic β-N (Ti–N) [6,13,20,21], while other strong peaks at 400 and 402.2 eV were assigned as molecularly chemisorbed γ-N_2 (N–H, N–N, N–O) [22,23], the one at 401.5 eV was attributed to the substitutional O–Ti–N sites in the TiO_2 lattice [24]. Therefore, all of the above results confirmed that N is not only successfully implanted in the structure but also present in a chemically bonded state (indicating that this type of N is the active doping species).

Fig. 5 shows the high-resolution S2p XPS spectra of NSTO, STO and TO. It could be observed that the S2p peak of NSTO contains two isolated weak peaks at binding energies of 168.1 and 162.8 eV, which can be attributed to the S^{6+} [9] and S^{2-} [8], respectively. There is only single peak at 168.1 eV in S2p region of STO. The S^{6+} may be assigned to the SO_4^{2-} ions adsorbed on the surface of NSTO and STO. The S^{2-} corresponds to the existence of Ti–S bond; it can be deduce that S atoms replaced O atoms in the TiO_2 lattice. It is the S^{2-} ions that replace the O^{2-} ions in the lattice of TiO_2, making it produce a lattice distort due to a large ionic radius difference between S^{2-} (0.184 nm) and O^{2-} (0.140 nm) [25]. Hence, its cell volume is enlarged. But the existence of adsorbing SO_4^{2-} does not change the unit cell parameters. This is why the unit cell parameters of STO are almost unchanged (see Table 1).

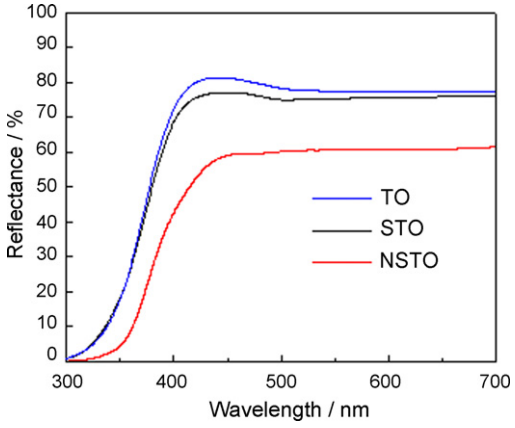

Fig. 2. UV–vis reflection spectra of the as-prepared TiO_2 powders.

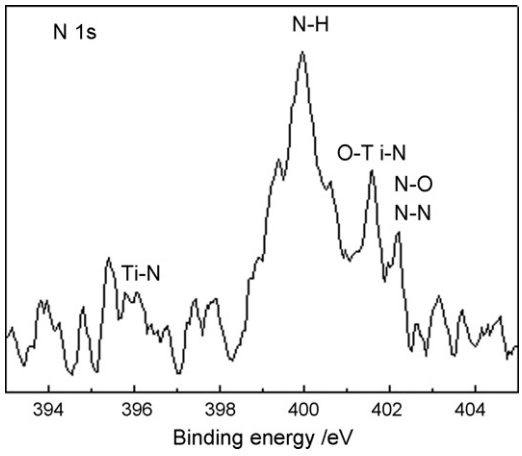

Fig. 4. High-resolution N1s XPS spectrum of NSTO.

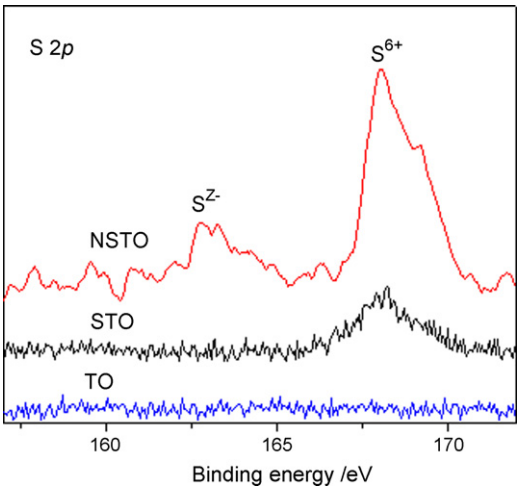

Fig. 5. High-resolution S2p XPS spectra of NSTO, STO and TO.

EA and XPS were used to determine the total N content, surface N content, respectively. The content of N (wt%) is 0.46% from EA and 0.504% from XPS, which indicates that for N dopant, the actual bulk N content is a little lower surface N content. It can be supposed that firstly N can be adsorbed mostly and strongly on the surface of NSTO due to its very large surface area, and then N may diffuse gradually into the bulk at given temperature and pressure during hydrothermal crystallization. Therefore, the content of N decreases from the exterior to the interior in the direction of the diffusion.

3.4. FT-IR spectra

The structure of sulfur and nitrogen complexes on the surface of TiO_2 was also examined by FT-IR measurements. Fig. 6 presents the FT-IR spectra of the samples ranging from 4000 to 400 cm^{-1}. The peak below 1000 cm^{-1} corresponds to the titania crystal lattice vibration. The broad peak at 3400 cm^{-1} corresponds to the O–H stretch region, whereas the peak at 1630 cm^{-1} results from the O–H bending of adsorbed water molecules. Two absorption peaks in the 900–1300 cm^{-1} region were observed on the spectra for NSTO and STO but absent on the one for the pure TiO_2. The peaks at 1135 and 1050 cm^{-1} were the characteristic frequencies of a bidentate SO_4^{2-} co-ordinated to metals such as Ti^{4+} [25,26]. Ammonium ions produced by the dissociation of thiourea were also found in the titania prepared using thiourea because of a peak at 1400 cm^{-1} attributable to the deformation mode of ammonium ions [27]. The result of FT-IR is in good agreement with XPS.

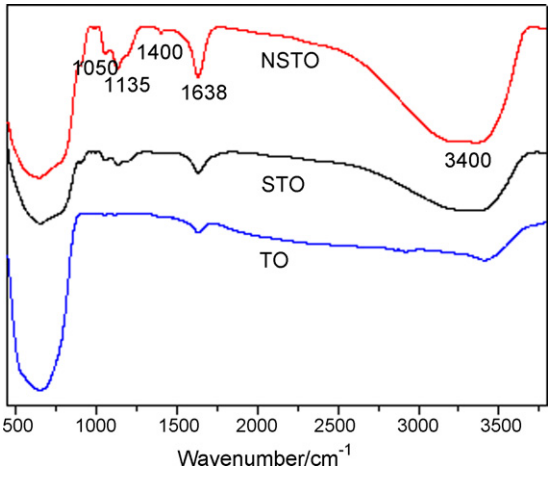

Fig. 6. FT-IR spectra of the as-prepared TiO_2 powders.

3.5. Photocatalytic activity

The photocatalytic activity was evaluated by measuring decomposition rates of methyl orange. However, the concentration of MO does not change using various as-prepared TiO_2 powders under dark condition. Illumination in the absence of TiO_2 powders does not result in the photocatalytic reaction. Therefore, the presence of both illumination and TiO_2 powders is necessary for the efficient degradation. Fig. 7 shows the photocatalytic activity of NSTO, STO and TO under UV and sunlight irradiation. It is obvious that the NSTO possessed the highest photocatalytic activity with the rate constant (k) about 0.267 h^{-1} under sunlight and 1.3854 h^{-1} under UV-light irradiation. For STO, under UV-light illumination the rate constant (1.0356 h^{-1}) is little higher than that of TO (0.9582 h^{-1}), but under sunlight illumination the rate constant (0.1938 h^{-1}) is higher than that of

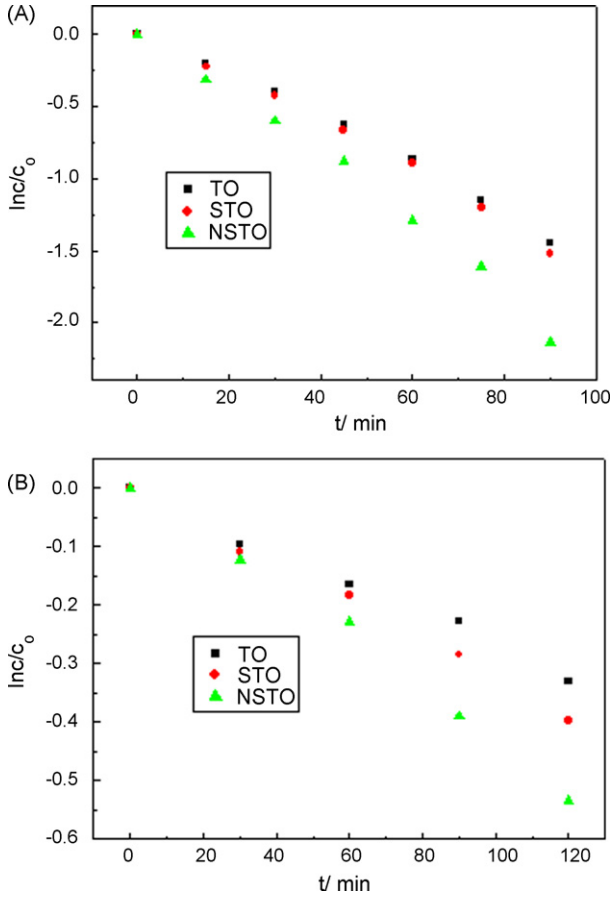

Fig. 7. Photocatalytic activity of the as-prepared photocatalysts under (A) UV-light and (B) sunlight irradiation (56 klx).

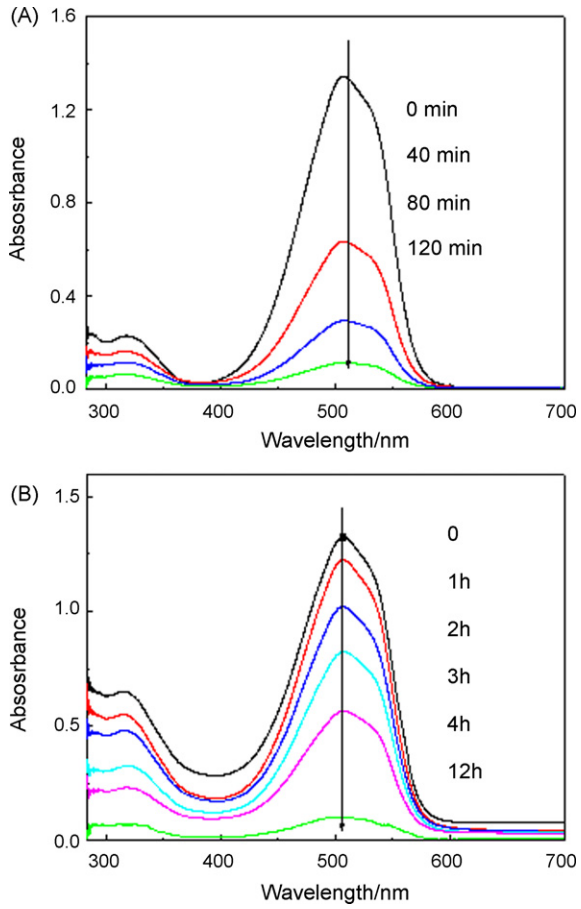

Fig. 8. UV–vis spectra profiles of MO after degradation in aqueous NSTO photocatalyst under UV (A) and sunlight (56 klx) (B) irradiation.

TO (0.1578 h^{-1}). TO displays the least photocatalytic activity. Moreover, for all samples, the rate constants of sunlight illumination are still lower than that of UV-light illumination. Fig. 8 shows the UV–vis spectra changes of methyl orange under visible and UV-light irradiation, which indicated that methyl orange had been not only degraded but also mineralized efficiently by NSTO.

Ohno et al. [9] reported that the activity of S-doped TiO_2 was higher than that of undoped TiO_2 only under irradiation at wavelengths longer than 440 nm. Our results confirmed that doping TiO_2 with S and N elements could enhance its response not only to the visible light but also to the UV light.

According to XPS, FT-IR and XRD results, it can be inferred that N and S were in situ codoped into the lattices of NSTO as in the forms of Ti–N, Ti–S, and molecularly chemisorbed γ-N_2 and SO_4^{2-}, whereas S in STO was in the form of the chemisorbed SO_4^{2-}. The adsorbed SO_4^{2-} enhanced the surface acidity and induced Brönsted acidic sites and Lewis acidic sites on the TiO_2 surface. These acidic sites could provide more surface chemisorption centers for reactants and oxygen molecules, also acted as electron acceptor, which would enhance the separation of photo-generated charge carriers and improve the photocatalytic efficiency [26]. So, STO shows a little better photocatalytic activity than TO under UV-light irradiation. Meanwhile, doped S also enhanced the absorption in vis-light region; this is why STO exhibits better performance than TO under sunlight irradiation. For NSTO, when TiO_2 is doped with S^{2-}, the mixing of the S3p states with VB increases the width of the valence band itself. This results in the lower energy shift in the optical absorption [8,28]. Furthermore, the doped N atoms can not only narrow the band gap of TiO_2 but also improve vis absorption, the photocatalytic activity of TiO_2 could be enhanced [7]. The UV–vis spectra in Fig. 2 unequivocally indicated that the N, S codoping did cause the narrowing of the band gap of TiO_2 because an obvious shift in the absorption edge of NSTO was observed, and did improve the absorbance in vis-light region. In addition, N doping resulted in the creation of surface oxygen vacancies (Ti/O <2.0). It is the oxygen-deficient sites formed in the grain-boundaries caused by N doping that contributed to the vis activity [12,29]. Consequently, the high UV and vis photocatalytic activity of NSTO is ascribed to a synergetic effect of doping N and S atoms.

4. Conclusion

Single anatase NSTO with good crystallinity can be successfully prepared by one-step hydrothermal method from a mixed aqueous solution of $Ti(SO_4)_2$ and thiourea. This method can efficiently dope sulfur and nitrogen elements into the lattice of TiO_2. The results show that NSTO exhibited an excellent photocatalytic activity no matter what light sources (UV or vis) were used. The high activity of NSTO is ascribed to a synergetic consequence of several beneficial effects such as the improvement in UV–vis absorption, good crystallization, the creation of surface oxygen vacancies and the enhancement of surface acidity induced by the N and S codoping.

Acknowledgements

The authors gratefully acknowledge the financial support from the National Natural Science Foundation of China (no. 40672027) and Anhui Province Foundation of Natural Science Research (no. 070414166).

References

[1] M.R. Hoffmann, S.T. Martin, W.Y. Choi, D.W. Bahnemann, Environmental applications of semiconductor photocatalysis, Chem. Rev. 95 (1995) 69–96.
[2] A. Mills, S. Lehunte, An overview of semiconductor photocatalysis, J. Photochem. Photobiol. A 108 (1997) 1–20.
[3] W. Choi, A. Termin, M.R. Hoffmann, The role of metal ion in quantum-sized TiO_2 correlation between photoreactivity and charge carrier recombination dynamics, J. Phys. Chem. 98 (1990) 13669–13679.
[4] P. Cheng, M. Zheng, Y. Jin, Q. Huang, M. Gu, Preparation and characterization of silica-doped titania photocatalyst through sol–gel method, Mater. Lett. 57 (2003) 2989–2994.
[5] K.V.S. Rao, B. Lavédrine, P. Boule, Influence of metallic species on TiO_2 for the photocatalytic degradation of dyes and dye intermediates, J. Photochem. Photobiol. A 154 (2003) 189–193.
[6] H. Irie, Y. Watanabe, K. Hashimoto, Carbon-doped anatase TiO_2 powders as a visible-light sensitive photocatalyst, Chem. Lett. 32 (2003) 772–773.
[7] R. Asahi, T. Morikawa, T. Ohwaki, K. Aoki, Y. Taga, Visible-light photocatalysis in nitrogen-doped titanium oxides, Science 293 (2001) 269–271.
[8] T. Umebayashi, T. Yamaki, H. Itoh, K. Asai, Band gap narrowing of titanium dioxide by sulfur doping, Appl. Phys. Lett. 81 (2002) 454–456.

[9] T. Ohno, M. Akiyoshi, T. Umebayashi, K. Asai, T. Mitsui, M. Matsumura, Preparation of S-doped TiO_2 photocatalysts and their photocatalytic activities under visible light, Appl. Catal. A 265 (2004) 115–121.

[10] J.C. Yu, J.G. Yu, W.K. Ho, Z. Jiang, L.Z. Zhang, Effects of F-doping on the photocatalytic activity and microstructures of nanocrystalline TiO_2 powders, Chem. Mater. 14 (2002) 3808–3816.

[11] D.M. Chen, D. Yang, Q. Wang, Z.Y. Jiang, Effects of boron doping on photocatalytic activity and microstructure of titanium dioxide nanoparticles, Ind. Eng. Chem. Res. 45 (2006) 4110–4116.

[12] D. Li, H. Haneda, S. Hishita, N. Ohashi, Visible-light-driven nitrogen-doped TiO_2 photocatalysts: effect of nitrogen precursors on their photocatalysis for decomposition of gas-phase organic pollutants, Mater. Sci. Eng. B 117 (2005) 67–75.

[13] D. Li, N. Ohashi, S. Hishita, T. Kolodiazhnyi, H. Haneda, Origin of visible-light-driven photocatalysis: a comparative study on N/F-doped and N–F-codoped TiO_2 powders by means of experimental characterizations and theoretical calculations, J. Solid State Chem. 178 (2005) 3293–3302.

[14] T. Ohno, T. Tsubota, Y. Nakamuraa, K. Sayama, Preparation of S, C cation-codoped $SrTiO_3$ and its photocatalytic activity under visible light, Appl. Catal. A 288 (2005) 74–79.

[15] S. Yin, K. Ihara, Y. Aita, M. Komatsu, T. Sato, Visible-light induced photocatalytic activity of $TiO_{2-x}A_y$ (A = N, S) prepared by precipitation route, J. Photochem. Photobiol. A 179 (2006) 105–114.

[16] H.Y. Liu, L. Gao, (Sulfur, nitrogen)-codoped rutile-titanium dioxide as a visible-light-activated photocatalyst, J. Am. Ceram. Soc. 87 (2004) 1582–1584.

[17] J.G. Yu, M.H. Zhou, B. Cheng, X.J. Zhao, Preparation, characterization and photocatalytic activity of in situ N,S-codoped TiO_2 powders, J. Mol. Catal. A 246 (2006) 176–184.

[18] K. Tanaka, T. Hisanaga, A.P. Riviera, D.F. Ollis, H. Al-Ekabi, Photocatalytic, Purification and Treatment of Water and Air, Elsevier, Amsterdam, 1993, pp. 169–178.

[19] C. Lettmann, K. Hildenbrand, H. Kisch, W. Macyk, W.F. Maier, Visible light photodegradation of 4-chlorophenol with a coke-containing titanium dioxide photocatalyst, Appl. Catal. B 32 (2001) 215–227.

[20] M. Miyauchi, A. Ikezawa, H. Tobimatsu, H. Iriea, K. Hashimoto, Zeta potential and photocatalytic activity of nitrogen doped TiO_2 thin films, Phys. Chem. Chem. Phys. 6 (2004) 865–870.

[21] H. Irie, Y. Watanabe, K. Hashimoto, Nitrogen-concentration dependence on photocatalytic activity of $TiO_{2-x}N_x$ powders, J. Phys. Chem. B 107 (2003) 5483–5486.

[22] M.C. Yang, T.S. Yang, M.S. Wong, Nitrogen-doped titanium oxide films as visible light photocatalyst by vapor deposition, Thin Solid Films 162 (2004) 469–470.

[23] Y. Suda, H. Kawasaki, T. Ueda, T. Ohshima, Preparation of high quality nitrogen doped TiO_2 thin film as a photocatalyst using a pulsed laser deposition method, Thin Solid Films 162 (2004) 453–454.

[24] Y.C. Hong, C.U. Bang, D.H. Shin, H.S. Uhm, Band gap narrowing of TiO_2 by nitrogen doping in atmospheric microwave plasma, Chem. Phys. Lett. 413 (2005) 454–457.

[25] R. Bacsa, J. Kiwi, T. Ohno, P. Albers, V. Nadtochenko, Preparation, testing and characterization of doped TiO_2 active in the peroxidation of biomolecules under visible light, J. Phys. Chem. B 109 (2005) 5994–6003.

[26] X.C. Wang, J.C. Yu, P. Liu, X.X. Wang, W.Y. Su, X.Z. Fu, Probing of photocatalytic surface sites on SO_4^{2-}/TiO_2 solid acids by in situ FT-IR spectroscopy and pyridine adsorption, J. Photochem. Photobiol. A 179 (2006) 339–347.

[27] L. Ren, X.T. Huang, F.L. Sun, X. He, Preparation and characterization of doped TiO_2 nanodandelion, Mater. Lett. 61 (2007) 427–431.

[28] T. Umebayashi, T. Yamaki, S. Tanala, K. Asai, Visible light-induced degradation of methylene blue on S-doped TiO_2, Chem. Lett. 32 (2003) 330–331.

[29] T. Ihara, M. Miyoshi, Y. Iriyama, O. Matsumoto, S. Sugihara, Visible-light-active titanium oxide photocatalyst realized by an oxygen-deficient structure and by nitrogen doping, Appl. Catal. B 42 (2003) 403–409.